

Diffuse myocardial fibrosis in adolescents operated with arterial switch for transposition of the great arteries - A CMR study[☆]



K.R. Suther^{a,*}, E. Hopp^a, O. Geier^b, H. Brun^c, B. Nguyen^a, A.H. Tomterstad^a, B. Smevik^a, A.E. Fiane^{d,e}, H.L. Lindberg^e, C. de Lange^a

^a Division of Radiology and Nuclear Medicine, Dept of Radiology, Rikshospitalet, Oslo University Hospital, Norway

^b Division of Radiology and Nuclear Medicine, Dept of Diagnostic Physics, Oslo University Hospital, Norway

^c Division of Paediatric and Adolescent Medicine, Dept of Paediatric Cardiology, Oslo University Hospital, Norway

^d Faculty of Medicine, University of Oslo, Norway

^e Dept. of Cardiothoracic Surgery, Oslo University Hospital, Norway

ARTICLE INFO

Article history:

Received 4 April 2018

Received in revised form 9 November 2018

Accepted 21 November 2018

Available online 22 November 2018

Keywords:

3.0 T

Cardiac magnetic resonance

Congenital heart defect

Fibrosis

MR relaxometry

Transposition of the great arteries

1. Introduction

In transposition of the great arteries (TGA), there is a ventricular-arterial discordance resulting in two independent circulatory systems incompatible with life unless a communication in-between them exists. The arterial switch operation (ASO) performed in the early neonatal period is the correction of choice [1,2]. However, there is some concern regarding the long-term outcome of the re-implanted coronary arteries,

and events such as asymptomatic coronary occlusion (with the risk of sudden cardiac death) have been reported [1,3,4]. Although rare, this emphasises the importance of and the need for follow-up of these patients, both regarding coronary artery patency and myocardial fibrosis [5–7]. In general, there is an excellent long-term outcome, and the incidence of focal fibrosis tends to be low in the ASO TGA [6,8]. Potential diffuse fibrosis, on the other hand, has only been evaluated in one very recent study to the best of our knowledge [9].

Myocardial fibrosis is a pathologic process that may be assessed with MRI, and it is defined by a significant increase in the collagen volume fraction of the myocardial tissue. There are different types of diffuse fibrosis: reactive interstitial, infiltrative interstitial and replacement fibrosis, but the first two may lead to replacement fibrosis [10]. The underlying pathology determines the distribution pattern, and late gadolinium enhancement (LGE) is a well-established, validated technique for detecting focal myocardial fibrosis [10–12].

To assess diffuse fibrosis, T1 mapping and extracellular volume (ECV) can be used, and several studies have showed good correlation between the collagen-volume fraction on biopsies compared to Gd-enhanced MRI both on 1.5 T and 3.0 T [13–15]. The clinical significance of T1 mapping and ECV is not entirely determined, but several recent articles have reviewed the different sequences and approaches available for determining the presence of diffuse fibrosis and their potential clinical utility [16–19].

In the case of congenital heart disease there are often residual and postoperative defects that may result in abnormal hemodynamics and possibly predispose for the development of diffuse fibrosis. Several studies have assessed the presence of diffuse myocardial fibrosis in both teenagers and adults with congenital heart disease (CHD), frequently finding increased cardiovascular MR (CMR) markers of diffuse fibrosis [9,20–25]. Available studies in the teenage group are focused on repaired Tetralogy of Fallot (ToF) and Fontan patients with only one recent study on pediatric ASO TGA patients. The latter revealed increased native T1 values while the ECV values were similar in patients and controls [9]. Two studies on ToF patients came from the same group and with their most recent larger data set they concluded that CMR markers of diffuse fibrosis in the left ventricle were not higher in this patient group as compared to controls [20,26], this was also

Abbreviations: ASO, arterial switch operation; BSA, body surface area; CHD, congenital heart disease; CMR, cardiovascular MR; CX, circumflex artery; ECG, electrocardiogram; ECV, extracellular volume fraction; EDVi, indexed end diastolic volume; EF, ejection fraction; Gd, gadolinium; Gd-FLASH, gadolinium enhanced fast low-angle shot; LAD, left anterior descending artery; LGE, late gadolinium enhancement; LV, left ventricle; MOLLI, modified look-locker; PACS, picture archive and communication system; PSIR, phase-sensitive inversion recovery; RCA, right coronary artery; ROI, region of interest; RV, right ventricle; SD, standard deviation; SSFP, steady state free precession; SVi, indexed stroke volume; TGA, transposition of the great arteries; ToF, Tetralogy of Fallot; VCG, vector-electrocardiogram; WH-CMRA, whole-heart coronary magnetic resonance angiography.

[☆] Trial registration: ClinicalTrials.gov: NCT01916499. Registered 2. August 2013.

* Corresponding author at: Division of Radiology and Nuclear Medicine, Paediatric Section, Oslo University Hospital, Rikshospitalet, PO box 4950, Nydalen, 0424 Oslo, Norway.

E-mail address: lensut@ous-hf.no (K.R. Suther).

confirmed by another study on ToF patients [27]. On the other hand, in a group of Fontan patients the single ventricles with right morphology had increased ECV and T1 relaxation time [23].

The purpose of this study was to assess focal and diffuse myocardial fibrosis as well as coronary origin patency in children/adolescents with ASO for TGA at 3.0 T MRI, hypothesizing that CMR markers of fibrosis is not increased in this patient group.

2. Materials and methods

The Norwegian South East Regional Committee for Medical and Health Research Ethics approved the study. All patients and their parents/carers and all healthy controls gave their written, informed consent to participation.

2.1. Subjects

Patients aged 9–15 years, operated with ASO for TGA in the neonatal period at our hospital were invited to this prospective study. Thirty consecutively chosen patients of both genders were enrolled from November 2013 through October 2014, and underwent whole-heart coronary magnetic resonance angiography (WH-CMRA) with both steady-state free precession (SSFP) and gadolinium-enhanced fast low-angle shot (Gd-FLASH), pre- and post-contrast T1 mapping by means of modified look-locker inversion recovery (MOLLI) and late gadolinium enhancement (LGE) as well as functional cine imaging. In addition, 15 healthy individuals aged 18–25 years of both genders underwent CMR with SSFP, pre- and post-contrast MOLLI and LGE from November 2014 to March 2015. All MRI exams were completed with the same software version and without general anaesthesia or any sedating drug. Blood was sampled prior to MRI on the day of examination in order to determine the haematocrit and creatinine values. The observers were blinded to the coronary artery pattern as well as the surgical report.

2.2. MRI protocol

The examinations were performed at a 3.0 T MR Skyra unit (Syngo D13, Siemens Healthineers, Erlangen, Germany) using an 18-channel body array coil combined with a 32-channel spine array coil. For gating purposes a 4-lead vector-electrocardiogram (VCG) was recorded, and respiratory navigation gating 2D PACE was used as well as cardiac shim. To assess the coronary arteries, two 3D volumes of the whole heart using respiratory-gated, fat saturated and ECG-triggered sequences were acquired; a balanced SSFP covering the whole thoracic cage (field of view 350 mm, reconstructed voxel size $0.8 \times 0.8 \times 1.0$ mm), and Gd-FLASH (field of view 320 mm, reconstructed voxel size $0.6 \times 0.6 \times 0.9$ mm) during intravenous injection of Gadoterate meglumine (Dotarem®, Guerbet, Villepinte, France) 0.4 ml/kg body weight, flow rate 0.15 ml/s, followed by an injection of 30 ml saline solution at similar flow rate. Fifteen seconds after initiating the injection of contrast media the Gd-FLASH scan was started, and went on to fulfill sampling after the completion of contrast agent and saline injection. The control group also received 0.4 ml/kg Gadoterate meglumine with the same flow rate and amount of saline for comparison reasons.

An ECG-gated, breath-hold MOLLI sequence in a 2-, 3- and 4-chamber view was used to measure the T1 times in diastole with a pre-contrast scheme 5(3)3 and a post-contrast scheme 4(1)3(1)2. Both MOLLI sequences had a field of view of 360 mm and reconstructed voxel size $1.9 \times 1.9 \times 8.0$ mm. Post-contrast MOLLI was performed at two time points after completion of contrast media administration; just before the LGE images approximately after 10 min, and after the LGE images. The LGE sequence was an ECG-gated, breath-hold, phase-sensitive inversion recovery (PSIR) gradient echo sequence with the inversion time selected to null the myocardial signal (field of view 330 mm, reconstructed voxel size $1.3 \times 1.3 \times 6.0$ mm) performed between 10 and 20 min after the intravenous administration of contrast media in 2-, 3-, 4-chamber and a 3D volume short axis view.

Standard long- and short axis cine (2D SSFP technique) were acquired for the assessment of ventricular volumetry in the patient group.

2.3. Image analysis

The evaluation of the coronary artery origins, pre- and post-contrast MOLLI images as well as visual inspection for presence of LGE was performed in the local picture archive and communication system (PACS; ISDN 17, Sectra, Linköping, Sweden) by two trained radiologists in consensus (with 7 and 14 years of CMR experience). Evaluation of the LGE images was done before post-processing the MOLLI images to avoid bias by including areas with known LGE in the T1 measurements.

T1 maps were generated on the scanner using motion corrected images. One region of interest (ROI) was drawn manually by the two observers within the myocardial borders in each of the expected coronary territories in the left ventricle (LV); right coronary artery (RCA), left anterior descending artery (LAD) and circumflex artery (CX), on a 2-chamber and 3-chamber view (Fig. 1). The ROI had a size of at least 23 mm^2 (>20 pixels), and a standard deviation $\leq 10\%$ was accepted. A ROI as large as possible was drawn in the blood pool within the ventricular lumen in a 2-chamber view avoiding the papillary muscles. This was done both on pre- and post-contrast MOLLI images enabling determination of native T1 values and the calculation of the extracellular volume fraction (ECV). ECV takes into

account the T1 behaviour of blood, varying dose and clearance of contrast material as well as haematocrit, and in this way, avoids confounders.

The ECV is given by the formula:

$$ECV = (1 - \text{hematocrit}) \times \frac{\frac{1}{T1_{\text{Myocardium post Gd}}} - \frac{1}{T1_{\text{Myocardium native}}}}{\frac{1}{T1_{\text{Blood post Gd}}} - \frac{1}{T1_{\text{Blood native}}}}$$

ECV divides the myocardium into a cellular and a matrix component permitting the calculation of cell and matrix volumes. For the patients total LV cell and matrix volumes were computed from the product of LV myocardial volume (LV mass divided by the specific gravity of myocardium (1.05 g/ml)) and (1-ECV) or ECV, respectively.

2.4. Statistical analysis

Normality of distribution was evaluated using the Kolmogorov-Smirnov's test. Continuously distributed variables are expressed by mean values, standard deviation (SD) in brackets and 95% confidence intervals calculated by the Student's procedure [28]. Independent sample *t*-test was used for the comparison of native T1 between the patient group and the healthy volunteers as well as for the comparison of late measurement ECV between the two groups. Comparisons of native T1 as well as ECV in the different expected coronary territories to each other in the patient group, were performed with paired sample *t*-test. SPSS version 24 was used for performing the analyses (SPSS Inc., Chicago, USA). *p*-Values < 0.05 were considered significant.

3. Results

Patient and control characteristics are given in Table 1. Volumetric measurements were performed in 29 patients, one patient was excluded due to insufficient image quality. As compared to normal values for gender and age according to Sarikouch et al., our group of patients had indexed values within the normal range for the LV except one borderline ejection fraction value, Table 1 [29]. Visual inspection revealed no areas of akinesia, hypokinesia or dyskinesia.

Of the included 30 patients a few image sets were incomplete (1 patient denied contrast media, 1 had missing creatinine value at the time of MR exam and did not receive contrast media, 1 patient had a minor post-contrast reaction with nausea and could not complete the CMR). One patient had a clear outlier native T1 value due to image artefacts, and in addition nine late post-contrast T1 maps for different patients were missing. None of the patients nor controls had a heart rate of >100 beats per minute. All individuals had normal creatinine value.

Native T1 relaxation time was significantly longer in the coronary territory of RCA in the control group, $p = 0.02$, while in the coronary territory of LAD there was borderline significant shorter native T1 time in the control group as compared to the patient group, $p = 0.05$ (Table 2).

Late measurement ECV (images 11–26 min after contrast media injection) was significantly higher in all the coronary territories in the patient group, $p \leq 0.03$ (Table 2). We did not find any significant difference in native T1 relaxation time between the genders in the patient group nor the controls, $p \geq 0.08$. Late measurement ECV showed significant lower value in males in the coronary territory of CX in both groups, $p = 0.03$ and $p = 0.02$, while in the control group there was significantly lower value in males in the coronary territory of RCA, $p = 0.04$.

The native T1 values were significantly shorter in the coronary territory of RCA than LAD and CX ($p = 0.01$ and $p = 0.02$) in the patient group, while late measurement ECV did not reveal any significant differences ($p \geq 0.07$). In the control group the native T1 values were significantly shorter in the coronary territory of LAD compared to RCA, $p = 0.04$, while late measurement ECV did not reveal any significant differences ($p \geq 0.09$). The boxplots in Fig. 2 illustrate an overlap of native T1 values and late ECV values when comparing the patient group and the control group, indicating that there are no cut-off values.

Images for early ECV calculation were performed too early in the healthy volunteers (images 4–9 min after contrast media injection) and could not be compared to the patient group (images 7–13 min after contrast media injection).

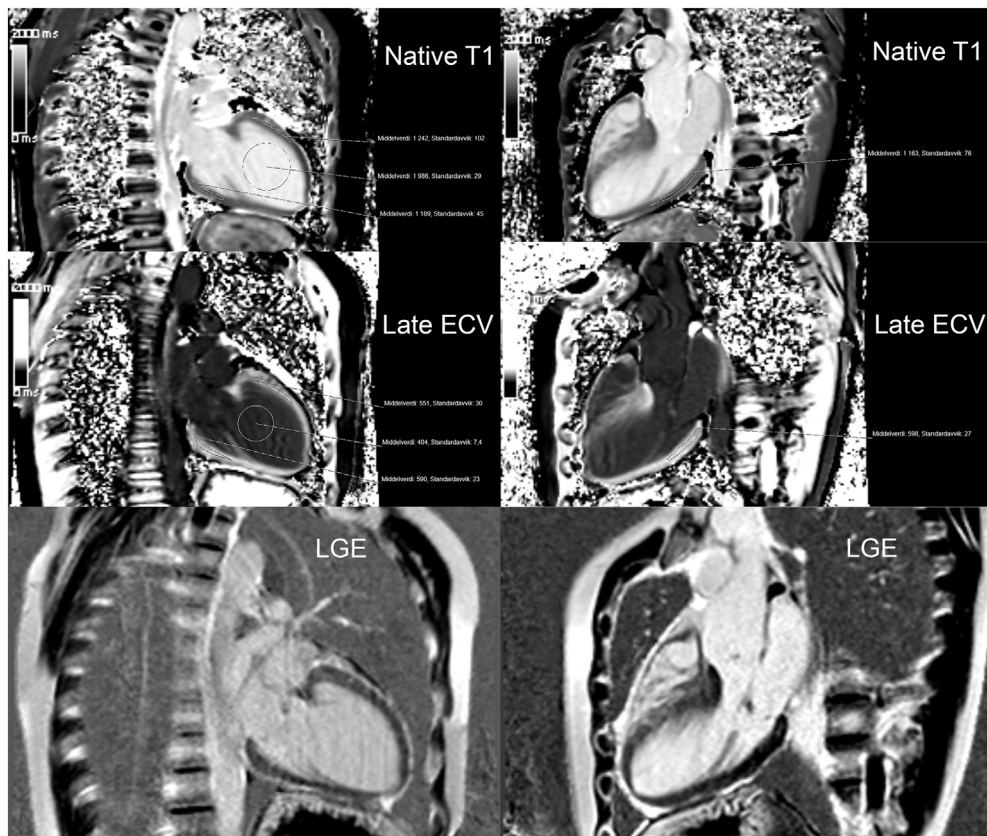


Fig. 1. T1 maps with regions of interest in 2- and 3-chamber view before and after contrast media (late measurement) in the expected coronary artery distribution areas. Late gadolinium enhancement images in 2- and 3-chamber view in the same individual.

The late measurement ECV was increased in the patients with a cell volume of 69.7%, 70.5% and 73.4% of the mean LV mass for RCA, LAD and CX respectively (Table 2).

Table 1
Patient demographics. Individual characteristics given in mean (SD) with min-max values.

	TGA	Healthy volunteers
No	30	15
Gender	21 male	7 male
Age, years	11.7 (1.9)	22.4 (2.5)
	9.3–15.3	18.6–25.8
Height, cm	150.8 (13.8)	176.1 (10.0)
	128–183	163–196
Weight, kg	43.5 (16.4)	73.5 (16.3)
	23–91	48–112
BSA, m ²	1.34 (0.30)	1.89 (0.25)
	0.90–2.15	1.47–2.42
Heart rate, beats per min	78 (13)	67 (10)
	50–100	50–86
Haematocrit	0.40 (0.03)	0.41 (0.03)
	0.36–0.45	0.37–0.46
Creatinine, µmol/l	45.9 (7.4)	69.7 (8.4)
	35–66	57–81
Left ventricle EDVi, ml/m ²	77.1 (14.4)	N/A
	57.1–104.8	
Left ventricle SVi, ml/m ²	51.1 (9.8)	N/A
	33.6–66.3	
Left ventricle EF, %	66.4 (5.9)	N/A
	51.1–76.9	
Left ventricle mVVi, g/m ²	48.9 (6.9)	N/A
	34.6–66.0	

BSA, body surface area; EDVi, end-diastolic volume indexed to body mass; SVi, stroke volume indexed to body mass; EF, ejection fraction; mVVi, muscle mass left ventricle indexed to body mass.

A normal pattern of the coronary arteries was found in 17 patients with RCA originating from the right coronary sinus and LAD and CX from the left coronary sinus. Seven patients had RCA and CX originating from the right coronary sinus and LAD from the left coronary sinus. The remaining 6 patients had different variants of coronary artery patterns, and among these CX could not be identified/evaluated in 2. However, there were no striking changes on native T1, early ECV, late ECV, LGE or regional function in the expected coronary territories in these 2 individuals. All the identified coronary arteries were without stenosis.

The four LGE acquisitions were obtained over a time-period of 3 min on average, between 10 and 20 min after contrast media administration, and there were no identified areas of LGE.

4. Discussion

We have demonstrated that children and adolescents treated with ASO for TGA had increased CMR derived ECV in all coronary territories that could indicate increased amount of left ventricular diffuse myocardial fibrosis when compared to young, healthy adults. While native T1 measurements were not able to uniformly discriminate between controls and patients. Furthermore, the patients presented with patent coronary artery ostias and without focal scarring. The volumetric measurements for the LV were within the normal range for gender and age [29].

The presence of a normal LV mass with increased ECV, but apparently preserved cellular mass in our patients, could indicate a primary fibroblast activation rather than myocyte loss [30,31]. This is in contrast to a study on adult atrial switch corrected TGA individuals that showed increased ECV in the subpulmonary LV accompanied by decreased LV mass [25]. Atrial switch is performed at an older age than the arterial switch procedure, and the difference in LV mass as compared to normal values suggest that the mechanism of fibrosis is different in these two

Table 2

Native T1 values, extracellular volume fraction (ECV), total left ventricular cell and matrix volumes in the expected coronary territories of the left ventricular wall. ECV is calculated from native T1 values, early and late post-contrast measurements given in mean (SD) with min–max values. Total left ventricular cell and matrix volumes are given in mean (SD).

		TGA	n	Controls	n	p-Value	
Native T1 ms, (SD)	RCA	1186 (65)	30	1234 (55)	15	0.02	
		1064–1270		1172–1371			
	LAD	1233 (52)	30	1198 (63)	15	0.05	
		1134–1349		1080–1301			
CX	1222 (60)	29	1211 (33)	15	0.53		
	1155–1388		1163–1268				
ECV %, (SD)	Early 10 min (7–13 min)	RCA	29 (4)	27	N/A	N/A	
			22–37				
		LAD	27 (4)	27	N/A	N/A	
			20–35				
		CX	26 (3)	26	N/A	N/A	
			16–32				
	Late 19 min (11–26 min)	RCA	30 (5)	24	26 (3)	15	0.02
			23–44		20–33		
		LAD	29 (5)	25	25 (3)	15	0.001
			18–43		19–29		
		CX	28 (5)	22	25 (3)	15	0.03
			16–43		19–32		
Cell volume ml, (SD)	RCA	46.7 (18.4)	23	N/A	N/A	N/A	
	LAD	47.2 (18.9)	24				
	CX	49.5 (19.6)	21				
Matrix volume ml, (SD)	RCA	19.7 (5.0)	23	N/A	N/A	N/A	
	LAD	18.3 (4.4)	24				
	CX	18.3 (4.3)	21				

TGA, transposition of the great arteries; n, number of individuals; ECV, extracellular volume fraction; RCA, right coronary artery; LAD, left anterior descending artery; CX, circumflex artery. Independent sample *t*-test with *p*-values ≤ 0.05 were considered statistically significant (bold).

groups. In a study by Broberg et al., the presence of increased left ventricular ECV and normal ejection fraction, another cardiac imaging biomarker, indicates that interstitial fibrosis might precede systolic dysfunction and could be an early biomarker [21]. A study of repaired ToF patients showed increased ECV to be associated with arrhythmia (LV) and right ventricular (RV) volume overload [22]. Riesenkampff et al. found that ToF patients as compared to controls, did not express higher CMR markers of diffuse fibrosis, however, cardiac dysfunction, a longer cardiopulmonary bypass time and increased aortic cross clamp time were associated with a higher LV native T1 times and ECV [26]. In our study the surgical report comprising information of the coronary artery pattern were not included.

Different pathophysiological mechanisms lead to myocardial fibrosis which is thought to be a part of myocardial remodelling [10]. One might speculate that the coronary artery re-implantation in ASO could cause an altered, insufficient hemodynamic flow to the myocardium with subsequent development of diffuse fibrosis. In almost all our patients we could identify the coronary artery origins without stenosis, and in the two cases with unidentified coronary artery origins we had no indirect findings suggesting serious coronary artery obstructions. There were no significant differences in late measurement ECV when comparing the different coronary territories neither in the patients nor controls which could support that the findings in our patients are related to the intrauterine hemodynamic condition in transposition of the great arteries.

In contrast to our findings, a study by Kawel et al. has shown significantly higher ECV in the septum of healthy volunteers compared to non-septal myocardium [32]. A previous study has shown significant variations in post-contrast T1 values in different parts of the myocardium in healthy children/teenagers as well as in children with ToF repair [20], but post-contrast T1 values are considered as an inferior marker of fibrosis compared to native T1 and ECV [16].

The recent study on a pediatric ASO TGA cohort found increased native T1 in the patient group while ECV was similar to controls, in contrast to our findings with increased ECV in the patient group [9]. Our mean ECV values are within the normal range for healthy middle aged adults, but the fact that they are significantly higher than in slightly older healthy young adults indicates the presence of tissue pathology

[33]. Several studies have shown that native T1 and ECV increase with age [34–36]. Another study found no age nor gender correlation to native T1, and one study found gender influence on native T1 and ECV and a slight decrease in native T1 with age, while yet another study found ECV to be slightly higher in healthy women than men, without correlation to age [33,37,38]. We found differences between genders in the late measurement ECV values both in the patient and control group, but this is probably related to a small sample size. Nevertheless, when dealing with low-magnitude pathologies, as in our patient group, normal ranges according to gender and to a lesser extent age are needed, but currently not available [39].

We did not find LGE in any of the patients, but LGE and T1 mapping are considered to reveal different pathophysiological entities. LGE is dependent on spatial heterogeneity and therefore not well suited to demonstrate the full spectrum of fibrosis [30].

In our study we used slow infusion of contrast media to optimise the CMRA, but earlier studies have shown that this does not affect the values of T1 mapping as long as the time interval after contrast media injection before T1 mapping acquisition is sufficient [35]. We performed the mapping sequence at two timepoints after Gd administration, and we found significantly higher ECV in all the coronary territories in the patient group late after completion of injection of contrast media (17–26 min). Stable results have been shown in two other studies 8.5–23.5 min and 12–50 min post-contrast, and the latest guidelines recommend post-contrast T1 mapping 10–30 min post-contrast administration [35,39,40].

5. Limitations

The age, BSA, gender ratio and heart rate differ between the patients and the healthy volunteers, and this makes the study not strictly prospective by definition. However, in order to administer intravenous contrast in healthy volunteers we had to recruit among young adults due to ethical considerations. This gave a difference in age, BSA and heart rate due to physiological differences between the groups, as expected. Heart rate does alter pre-contrast T1, and this could be a potential limitation although none of the patients nor controls had a heart rate above 100 bpm [41]. However, the slight difference in heart rate is most likely

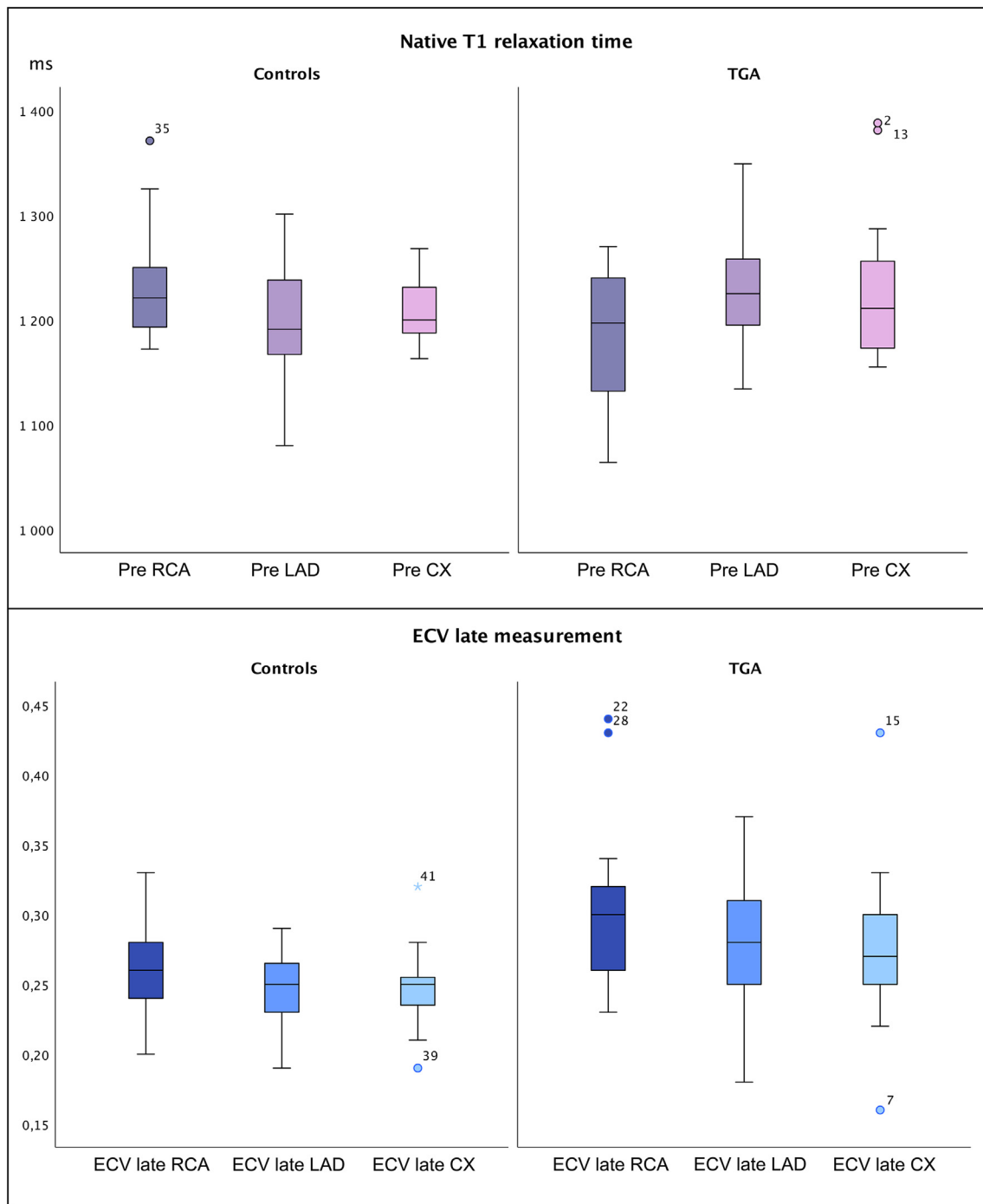


Fig. 2. Boxplot for the three coronary artery distribution areas, comparison between patients operated with arterial switch for transposition of the great arteries (TGA) and controls. ms, milliseconds; ECV, extracellular volume fraction; Pre RCA, native T1 relaxation time in the right coronary artery territory; Pre LAD, native T1 relaxation time in the left anterior descending artery territory; Pre CX, native T1 relaxation time in the circumflex artery territory; ECV late RCA, extracellular volume fraction late measurement in the right coronary artery territory; ECV late LAD, extracellular volume fraction late measurement in the left anterior descending artery territory; ECV late CX, extracellular volume fraction late measurement in the circumflex artery territory.

not a major contributor to the difference in native T1 and ECV seen between the groups [42].

There is also a difference in gender distribution in the patient group, but we invited all ASO TGA patients operated in our hospital to participate, and there is a male predominance in this cohort.

In our study we have used a 2-, 3- and 4-chamber view for T1 mapping sequences, but according to the latest clinical recommendations for CMR mapping of T1, T2, T2* and ECV by the Society for Cardiovascular Magnetic resonance (SCMR), two or several short axis maps should be used in addition to one or several long axis maps for T1 mapping [39].

A previous study has shown no statistically significant difference in T1 values when comparing short and long axis measurements, and this was the rationale for choosing the long axis views in our study [43].

The recommended dose of Gadolinium based contrast is 0.1–0.2 mmol/kg for T1 mapping and ECV measurements, and our patients received 0.2 mmol/kg in order to optimise the CMRA and the same amount was administered to the healthy volunteers for comparison reasons. This could be a potential source of error as it was shown in a study by Dabir et al. that the ECV values were dose dependent in the range of 0.1–0.2 mmol/kg [33].

The ROIs were traced within the myocardial borders according to the recommendations, but this has the potential of overlooking abnormal values due to ischemic changes [39]. As we did not find any LGE in our patient group this potential error seems unlikely in our study.

Histological validation of the MOLLI sequence was not performed on the participants in this study, and as a consequence we cannot be certain that our findings represent diffuse myocardial fibrosis. On the other hand, in the absence of myocardial inflammation and infarction, the most likely explanation of our findings of increased ECV in the patient group is diffuse myocardial fibrosis based on validation of the sequence in other cohorts.

Unfortunately, there was a difference in timing of the early post-contrast acquisitions for ECV calculations in the controls versus the patients, and a comparison between the two groups could not be made.

The drawings on the T1 maps were performed by two observers in a very standardized fashion, and preceded by a consensus reading to avoid inaccuracies, but no intra- nor inter-observer variation was tested.

Finally, the role of T1 mapping and ECV in CHD is not clarified [17], and the clinical importance of our findings is uncertain. However, T1 mapping offers a clear advantage in the tissue characterization compared to biopsy with the non-invasive ability to characterize the whole myocardium as well as its potential for individual follow-up. Further studies are needed to decide whether our findings are reproducible, represent a developing condition, and if this potentially could cause cardiac dysfunction later in life.

6. Conclusions

Our young TGA patients operated with ASO had increased CMR derived ECV in otherwise healthy hearts, with no pathology in the coronary artery origins. Longitudinal studies are required to test the clinical and prognostic significance of these findings, that might indicate the presence of diffuse myocardial fibrosis. Thus, MR relaxometry might be an important addition in the surveillance of the ASO TGA patient group.

Declarations of interest

None.

Declarations

Consent for publication

All subjects, both patients and healthy controls, and the patients' parents/carers gave their written, informed consent to participation and publication of the data, and images used are entirely unidentifiable.

Availability of data and material

The datasets used/analysed during the current study is available from the corresponding author on reasonable request.

Competing interests

The authors declare that they have no competing interests. No disclosures.

Acknowledgement

We thank Siemens for providing the quantitative cardiac parameter mapping work-in-progress package used in this study.

Funding

Financial support was given by the Norwegian Lung and Heart Association, Professor K V Halls Foundation, Inger R. Haldorsens Foundation, Renee and Bredo Grimsgaards Foundation and the Norwegian Society of Radiology for participants' travel expenses and costs related to the MRI exams.

References

- [1] J. Losay, A. Touchot, A. Serraf, A. Litvinova, V. Lambert, J.D. Piot, et al., Late outcome after arterial switch operation for transposition of the great arteries, *Circulation* 104 (2001).
- [2] P. Khairy, M. Clair, S.M. Fernandes, E.D. Blume, A.J. Powell, J.W. Newburger, et al., Cardiovascular outcomes after the arterial switch operation for D-transposition of the great arteries, *Circulation* 127 (3) (2013) 331–339.
- [3] P.A. Hutter, G.B. Bennink, L. Ay, I.B. Raes, J.F. Hitchcock, E.J. Meijboom, Influence of coronary anatomy and reimplantation on the long-term outcome of the arterial switch, *Eur. J. Cardiothorac. Surg.* 18 (2) (2000) 207–213.
- [4] A. Legendre, J. Losay, A. Touchot-Kone, A. Serraf, E. Belli, J.D. Piot, et al., Coronary events after arterial switch operation for transposition of the great arteries, *Circulation* 108 (Suppl. 1) (2003) II186–90.
- [5] M.S. Cohen, B.W. Eidem, F. Cetta, M.A. Fogel, P.C. Frommelt, J. Ganame, et al., Multimodality imaging guidelines of patients with transposition of the great arteries: a report from the American Society of Echocardiography developed in collaboration with the Society for Cardiovascular Magnetic Resonance and the Society of Cardiovascular Computed Tomography, *J. Am. Soc. Echocardiogr.* 29 (7) (2016) 571–621.
- [6] D. Tobler, M. Motwani, R.M. Wald, S.L. Roche, F. Verocai, R.M. Iwanochko, et al., Evaluation of a comprehensive cardiovascular magnetic resonance protocol in young adults late after the arterial switch operation for d-transposition of the great arteries, *J. Cardiovasc. Magn. Reson.* 16 (1) (2014) 98.
- [7] A. Kempny, K. Wustmann, F. Borgia, K. Dimopoulos, A. Uebing, W. Li, et al., Outcome in adult patients after arterial switch operation for transposition of the great arteries, *Int. J. Cardiol.* 167 (2013).
- [8] B. Manso, A. Castellote, L. Dos, J. Casaldaliga, Myocardial perfusion magnetic resonance imaging for detecting coronary function anomalies in asymptomatic paediatric patients with a previous arterial switch operation for the transposition of great arteries, *Cardiol. Young* 20 (2010).
- [9] H.B. Grotenhuis, B. Cifra, L.L. Mertens, E. Riessenkampff, C. Manlihot, M. Seed, et al., Left ventricular remodelling in long-term survivors after the arterial switch operation for transposition of the great arteries, *Eur. Heart J. Cardiovasc. Imaging* (2018) [Epub ahead of print].
- [10] N. Mewton, C.Y. Liu, P. Croisille, D. Bluemke, J.A. Lima, Assessment of myocardial fibrosis with cardiovascular magnetic resonance, *J. Am. Coll. Cardiol.* 57 (8) (2011) 891–903.
- [11] R.J. Kim, D.S. Fieno, T.B. Parrish, K. Harris, E.L. Chen, O. Simonetti, et al., Relationship of MRI delayed contrast enhancement to irreversible injury, infarct age, and contractile function, *Circulation* 100 (19) (1999) 1992–2002.
- [12] R.J. Kim, T.S. Albert, J.H. Wible, M.D. Elliott, J.C. Allen, J.C. Lee, et al., Performance of delayed-enhancement magnetic resonance imaging with gadoversetamide contrast for the detection and assessment of myocardial infarction: an international, multicenter, double-blinded, randomized trial, *Circulation* 117 (5) (2008) 629–637.
- [13] C.T. Sibley, R.A. Noureldin, N. Gai, M.S. Nacif, S. Liu, E.B. Turkbey, et al., T1 mapping in cardiomyopathy at cardiac MR: comparison with endomyocardial biopsy, *Radiology* 265 (3) (2012) 724–732.
- [14] L. Iles, H. Pfluger, A. Phrommintikul, J. Cherayath, P. Aksit, S.N. Gupta, et al., Evaluation of diffuse myocardial fibrosis in heart failure with cardiac magnetic resonance contrast-enhanced T1 mapping, *J. Am. Coll. Cardiol.* 52 (19) (2008) 1574–1580.
- [15] C. de Meester de Ravenstein, C. Bouzin, S. Lazam, J. Boulif, M. Amzulescu, J. Melchior, et al., Histological validation of measurement of diffuse interstitial myocardial fibrosis by myocardial extravascular volume fraction from Modified Look-Locker imaging (MOLLI) T1 mapping at 3 T, *J. Cardiovasc. Magn. Reson.* 17 (2015) 48.
- [16] J.C. Moon, D.R. Messroghli, P. Kellman, S.K. Piechnik, M.D. Robson, M. Ugander, et al., Myocardial T1 mapping and extracellular volume quantification: a Society for Cardiovascular Magnetic Resonance (SCMR) and CMR Working Group of the European Society of Cardiology consensus statement, *J. Cardiovasc. Magn. Reson.* 15 (2013) 92.
- [17] S. Ghoni, I. Voges, P.D. Gatehouse, J. Keegan, M.A. Gatzoulis, P.J. Kilner, et al., Myocardial architecture, mechanics, and fibrosis in congenital heart disease, *Front. Cardiovasc. Med.* 4 (2017) 30.
- [18] E. Riessenkampff, D.R. Messroghli, A.N. Redington, L. Grosse-Wortmann, Myocardial T1 mapping in pediatric and congenital heart disease, *Circ. Cardiovasc. Imaging* 8 (2) (2015), e002504.
- [19] A.J. Taylor, M. Salerno, R. Dharmakumar, M. Jerosch-Herold, T1 mapping: basic techniques and clinical applications, *JACC Cardiovasc. Imaging* 9 (1) (2016) 67–81.
- [20] M.F. Kozak, A. Redington, S.J. Yoo, M. Seed, A. Greiser, L. Grosse-Wortmann, Diffuse myocardial fibrosis following tetralogy of Fallot repair: a T1 mapping cardiac magnetic resonance study, *Pediatr. Radiol.* 44 (4) (2014) 403–409.
- [21] C.S. Broberg, S.S. Chugh, C. Conklin, D.J. Sahn, M. Jerosch-Herold, Quantification of diffuse myocardial fibrosis and its association with myocardial dysfunction in congenital heart disease, *Circ. Cardiovasc. Imaging* 3 (6) (2010) 727–734.

- [22] C.A. Chen, S.M. Dusenbery, A.M. Valente, A.J. Powell, T. Geva, Myocardial ECV fraction assessed by CMR is associated with type of hemodynamic load and arrhythmia in repaired tetralogy of Fallot, *JACC Cardiovasc. Imaging* 9 (1) (2016) 1–10.
- [23] A. Kato, E. Riesenkampff, D. Yim, S.J. Yoo, M. Seed, L. Grosse-Wortmann, Pediatric Fontan patients are at risk for myocardial fibrotic remodeling and dysfunction, *Int. J. Cardiol.* 240 (2017) 172–177.
- [24] C.M. Plymen, D.M. Sado, A.M. Taylor, A.P. Bolger, P.D. Lambiase, M. Hughes, et al., Diffuse myocardial fibrosis in the systemic right ventricle of patients late after Mustard or Senning surgery: an equilibrium contrast cardiovascular magnetic resonance study, *Eur. Heart J. Cardiovasc. Imaging* 14 (10) (2013) 963–968.
- [25] N. Shehu, C. Meierhofer, D. Messroghli, N. Mkrtychyan, S. Martinoff, P. Ewert, et al., Diffuse fibrosis is common in the left, but not in the right ventricle in patients with transposition of the great arteries late after atrial switch operation, *Int. J. Cardiovasc. Imaging* 34 (8) (2018) 1241–1248.
- [26] E. Riesenkampff, W. Luining, M. Seed, P. Chungsomprasong, C. Manlihot, B. Elders, et al., Increased left ventricular myocardial extracellular volume is associated with longer cardiopulmonary bypass times, biventricular enlargement and reduced exercise tolerance in children after repair of tetralogy of Fallot, *J. Cardiovasc. Magn. Reson.* 18 (1) (2016) 75.
- [27] D. Yim, E. Riesenkampff, P. Caro-Dominguez, S.J. Yoo, M. Seed, L. Grosse-Wortmann, Assessment of diffuse ventricular myocardial fibrosis using native T1 in children with repaired tetralogy of Fallot, *Circ. Cardiovasc. Imaging* 10 (3) (2017).
- [28] D.G. Altman, *Practical Statistics for Medical Research*, Chapman and Hall, London, 1991.
- [29] S. Sarikouch, B. Peters, M. Gutberlet, B. Leismann, A. Kelter-Kloeping, H. Koerperich, et al., Sex-specific pediatric percentiles for ventricular size and mass as reference values for cardiac MRI: assessment by steady-state free-precession and phase-contrast MRI flow, *Circ. Cardiovasc. Imaging* 3 (1) (2010) 65–76.
- [30] E.B. Schelbert, D.R. Messroghli, State of the art: clinical applications of cardiac T1 mapping, *Radiology* 278 (3) (2016) 658–676.
- [31] T.A. Treibel, R. Kozor, R. Schofield, G. Benedetti, M. Fontana, A.N. Bhuva, et al., Reverse myocardial remodeling following valve replacement in patients with aortic stenosis, *J. Am. Coll. Cardiol.* 71 (8) (2018) 860–871.
- [32] N. Kawel, M. Nacif, A. Zavodni, J. Jones, S. Liu, C.T. Sibley, et al., T1 mapping of the myocardium: intra-individual assessment of the effect of field strength, cardiac cycle and variation by myocardial region, *J. Cardiovasc. Magn. Reson.* 14 (2012) 27.
- [33] D. Dabir, N. Child, A. Kalra, T. Rogers, R. Gebker, A. Jabbour, S. Plein, C. Yu, J. Otton, A. Kidambi, A. McDiarmid, D. Broadbent, D. Higgins, B. Schnackenburg, L. Foote, C. Cummins, E. Nagel, V. Puntmann, Reference values for healthy human myocardium using a T1 mapping methodology: results from the International T1 multicenter cardiovascular magnetic resonance study, *J. Cardiovasc. Magn. Reson.* 16 (2014) 69 <http://jcmr-online.com/content/16/1/69>.
- [34] C.Y. Liu, Y.C. Liu, C. Wu, A. Armstrong, G.J. Volpe, R.J. van der Geest, et al., Evaluation of age-related interstitial myocardial fibrosis with cardiac magnetic resonance contrast-enhanced T1 mapping: MESA (Multi-Ethnic Study of Atherosclerosis), *J. Am. Coll. Cardiol.* 62 (14) (2013) 1280–1287.
- [35] E.B. Schelbert, S.M. Testa, C.G. Meier, W.J. Ceyrolles, J.E. Levenson, A.J. Blair, et al., Myocardial extravascular extracellular volume fraction measurement by gadolinium cardiovascular magnetic resonance in humans: slow infusion versus bolus, *J. Cardiovasc. Magn. Reson.* 13 (2011) 16.
- [36] M. Ugander, A.J. Oki, L.Y. Hsu, P. Kellman, A. Greiser, A.H. Aletras, et al., Extracellular volume imaging by magnetic resonance imaging provides insights into overt and sub-clinical myocardial pathology, *Eur. Heart J.* 33 (10) (2012) 1268–1278.
- [37] D.M. Sado, A.S. Flett, S.M. Banypersad, S.K. White, V. Maestrini, G. Quarta, et al., Cardiovascular magnetic resonance measurement of myocardial extracellular volume in health and disease, *Heart* 98 (19) (2012) 1436–1441.
- [38] S. Rosmini, H. Bulluck, T.A. Treibel, A. Abdel-Gadir, A.N. Bhuva, V. Culotta, A. Merghani, V. Maestrini, A.S. Herrey, P. Kellman, C. Manisty, J. Moon, Native myocardial T1 and ECV with age and gender developing normal reference ranges – a 94 healthy volunteer study, *J. Cardiovasc. Magn. Reson.* 18 (Suppl. 1) (2016) O42.
- [39] D.R. Messroghli, J.C. Moon, V.M. Ferreira, L. Grosse-Wortmann, T. He, P. Kellman, et al., Clinical recommendations for cardiovascular magnetic resonance mapping of T1, T2, T2* and extracellular volume: a consensus statement by the Society for Cardiovascular Magnetic Resonance (SCMR) endorsed by the European Association for Cardiovascular Imaging (EACVI), *J. Cardiovasc. Magn. Reson.* 19 (1) (2017) 75.
- [40] J.J. Lee, S. Liu, M.S. Nacif, M. Ugander, J. Han, N. Kawel, et al., Myocardial T1 and extracellular volume fraction mapping at 3 Tesla, *J. Cardiovasc. Magn. Reson.* 13 (2011) 75.
- [41] P. Kellman, M.S. Hansen, T1-mapping in the heart: accuracy and precision, *J. Cardiovasc. Magn. Reson.* 16 (2014) 2.
- [42] V.S. Vassiliou, E.L. Heng, P.D. Gatehouse, J. Donovan, C.E. Raphael, S. Giri, et al., Magnetic resonance imaging phantoms for quality-control of myocardial T1 and ECV mapping: specific formulation, long-term stability and variation with heart rate and temperature, *J. Cardiovasc. Magn. Reson.* 18 (1) (2016) 62.
- [43] M.S. Nacif, E.B. Turkbey, N. Gai, S. Nazarian, R.J. van der Geest, R.A. Noureldin, et al., Myocardial T1 mapping with MRI: comparison of look-locker and MOLLI sequences, *J. Magn. Reson. Imaging* 34 (6) (2011) 1367–1373.